SF2A 2007
J. Bouvier, A. Chalabaev, C. Charbonnel (eds)

HYDRODYNAMIC SIMULATIONS OF IRRADIATED SECONDARIES IN DWARF NOVAE

M. Viallet[1] and J.-M. Hameury[1]

Abstract. Secondary stars in dwarf novae are strongly irradiated during outbursts. We present here numerical simulations of the surface flow on the secondary star that results from its inhomogenious heating by the accretion luminosity. We show that a circulation flow toward the L_1 point forms at the beginning of an outburst and thus provides a natural way to transport heat and matter. However, the Lagrangian point region is not efficiently heated this way due to the short cooling time scale of the hot matter as it enters the region shaded by the accretion disc. We discuss implication for a possible mass transfer enhancement.

1 Introduction

Dwarf novae (DN) are cataclysmic variables that undergo outbursts, i.e. a sudden increase of their luminosity by a few magnitudes lasting for a few days (see e.g. Warner 1995 for a review). In the current picture, outbursts are due to a thermal/viscous instability of the accretion disc. The accretion disc undergoes a limit cycle between outburst phases of high accretion rate and quiescence phases of low accretion rate where the disc re-builds (see Cannizzo 1993; Lasota 2001 for reviews). The role of the irradiation of the secondary star during an outburst is still a matter of debate.

During an outburst, the irradiation flux impinging the secondary exceeds by a large amount the intrinsic stellar flux (Smak 2004a). It has been often argued that it could somehow result in a substantial enhancement of the mass transfer rate, but observational evidences for such episodes remains polemical (see Osaki & Meyer 2003; Smak 2004b). Still, mass transfer enhancement episodes are sometimes introduced in outburst models to explain some DN behavior (e.g. superoutbursts of SU UMa stars).

The L_1 point is shaded by the accretion disc and is therefore not under the direct influence of irradiation. Smak (2004a) investigated the possibility of a circulation flow transporting heat from irradiated regions towards the L_1 point and found substantial enhancement of the mass transfer rate. Smak's results were challenged by Osaki & Meyer (2004, see Smak 2004b for a response to their criticism), who argue that no flow can reach the L_1 point as a result of the strong deflection by the Coriolis force.

These studies were based on the assumption of steady state and/or one dimensional arguments (c.f. Osaki & Meyer). Here we fully account for intrinsic two-dimensional and time dependent nature of the problem.

2 Model and numerical code

We give here an overview of our model and numerical code. For more details, we refer the reader to Viallet & Hameury (2007). We compute the surface flow on the secondary by solving numerically the Euler equations. The variables that enter the equations are Σ, the surface density, $\vec{v}$, the surface velocity and P, the vertically averaged pressure. The most important dynamical ingredient of the problem is the Coriolis force, which is strong in these short period systems. In our 2D approach, only its component parallel to the surface enters the equations and its magnitude is fv where v is the velocity and $f = 2\vec{\Omega}.\vec{n}$ is the "Coriolis parameter" ($\vec{\Omega}$ is the rotation vector of the secondary, $\vec{n}$ is the normal to the surface). Due to the shape of the Roche lobe, this parameter has a singular behavior in the L_1 region, as seen on the left panel of Fig. 1. As stressed by Osaki &

[1] Observatoire de Strasbourg, Universit Louis Pasteur/CNRS, 11, rue de l'universit, Strasbourg

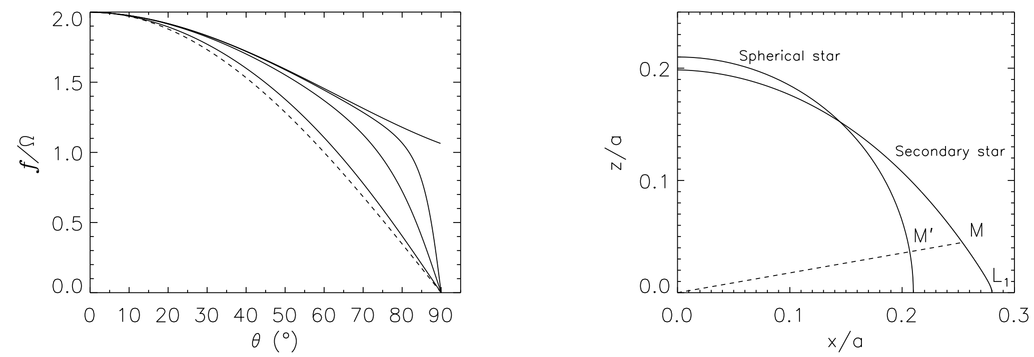

Fig. 1. Left panel: profile of f along meridians at longitude $0°$ (L_1 meridian), $5°$, $15°$ and $45°$ (from top to bottom). For comparison the profile corresponding to spherical geometry is also shown in dashed line. Right panel: mapping from the Roche lobe onto a spherical star. The radius of the spherical star is the mean-radius of the Roche lobe (see e.g. Warner 1995).

Meyer (2003), contrary to spherical geometry, f does not vanish as one approaches L_1 on the main meridian. However, as one moves away from L_1 in longitude, f vanishes rapidly as one recover a spherical like geometry.

For simplicity we have considered here a *spherically geometric* star on which we apply a position dependent Coriolis parameter (and hence of Coriolis force) computed from the Roche geometry. There is therefore no need to use complicated curvilinear coordinates (Kopal 1969) to describe the surface of the secondary. It should be noted that the distance between the shadow boundary and the L_1 point is smaller in our model than in the real Roche geometry (see right panel of Fig. 1).

We consider an outburst lasting 60 orbital periods, i.e. a few days, with a rapid raise and decay (the exact temporal profile is not of first importance for our purpose). At the outburst maximum, the irradiation flux impinging the secondary corresponds to an effective temperature of 10^4 K. We assume that the irradiation flux is reprocessed below the photosphere and is thus re-radiated as a black body (a more detailed treatment of radiative transfer in the secondary atmosphere is beyond the scope this study). Irradiation thus enters our energy equation via a heating term $Q^+(\theta, \phi, t)$. The spatial dependence accounts for oblique incidence and shadowing by the accretion disc (see below) and the time dependence accounts for the outburst profile. The radiative cooling term is $Q^- = \sigma T^4$ (T is the temperature of the gas).

The profile of the shadow casted on the secondary by the disc is computed by looking if the running point on the secondary can see the primary for a given aperture of the disc. We use the numerical code from Hameury et al. (1998) to compute the structure of the disc during outbursts. This yields aperture of the order of $4° - 6°$ which translates into a shadow boundary located at $\theta \sim 80°$ when measured on the main meridian of the secondary (see Viallet & Hameury for more details).

We use the TVD-MacCormack scheme (Yee 1987) to solve numerically the Euler equations with the source terms described above (Coriolis force in the momentum equation + cooling/heating terms in the energy equation). This is an explicit two step (predictor/corrector) scheme enabling second order accuracy in space and time. In addition, a TVD (Total Variation Diminishing) step is performed in order to prevent non physical oscillation to grow in strong gradient region. The TVD step acts as adding a "selective" numerical dissipation. Since spherical coordinates are singular at their poles, we exclude two small polar caps from the domain of integration. This has been checked to not influence the results, as there is not much dynamic near the poles which are not illuminated. The boundary conditions corresponds to free outflow near the poles and periodicity in the longitudinal direction.

3 Results

Fig. 2 shows snapshots of a typical simulation at the beginning of an outburst ($t = 0.7\ P_{\rm orb}$), at the outburst maximum ($t = 30\ P_{\rm orb}$) and during the outburst decay ($t = 45\ P_{\rm orb}$). At the beginning of the outburst, irradiation raises the temperature and hence the pressure on the secondary. The pressure gradient drives the

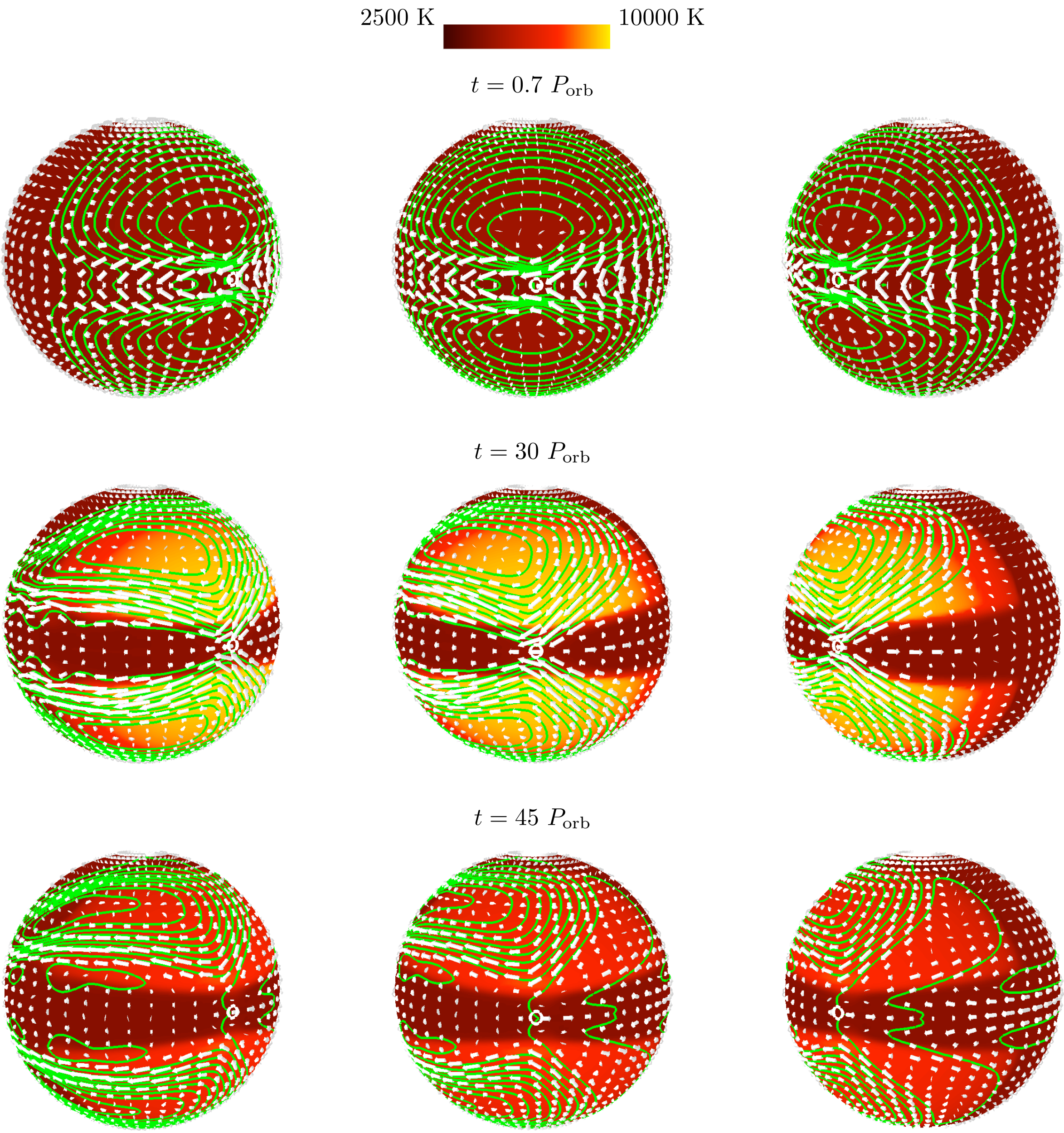

Fig. 2. Snapshots at $t = 0.7, 30, 45\ P_{\rm orb}$. Each snapshot shows the color coded temperature field (see the color legend), isobars and the velocity field. The central panel shows the secondary face on; in the left and right panels, the secondary is rotated by +/- 30 degrees. The L_1 region is marked by a circle whose surface is equal to the stream cross section (see Eq. (17)). For the sake of figure readability, the magnitude of the velocity field has been multiplied by 6 at $t = 0.7\ P_{\rm orb}$.

flow towards the equator and is strongly deflected by the Coriolis force. The deflection is strongest on the L_1 meridian (see middle panel at $t = 0.7\ P_{\rm orb}$). This leads to an oscillatory pattern of the velocity field which drives the flow toward he L_1 point. At later times (see snapshots at $t = 30\ P_{\rm orb}$), an anticyclonic perturbation has formed as a result of irradiation (the same happens by symmetry on the southern hemisphere). The circulation flow associated with this high pressure region is “geostrophic”, i.e. the Coriolis force balances the pressure gradient (see Pedlosky 1982). This circulation flow crosses the L_1 region as a result of the dynamical adjustment occurring at the very beginning of the outburst and described above.

However, the anticyclonic perturbation slowly drifts westward during the outburst and, as a consequence,

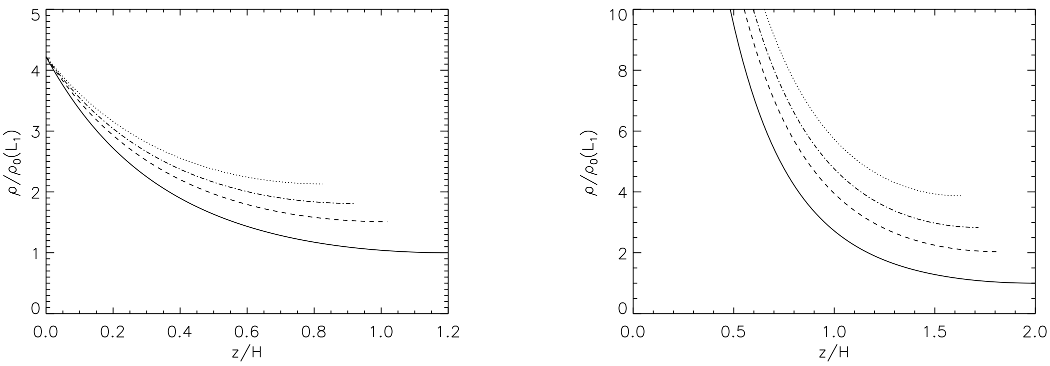

Fig. 3. Vertical profile of the density ρ in an isothermal atmosphere when $v_\parallel = 0,\ 0.5c_s,\ 0.75c_s$ (from bottom to top) for $z_{L_1}/H = 1.2$ (left panel) and $z_{L_1}/H = 2$ (right panel). The density is normalized by the density at L_1 when $v_\parallel = 0$.

the circulation flow moves away from the L_1 region. Our simulation shows that the circulation flow crosses L_1 approximatively only during the first half of the outburst. The maximum velocity is reached at L_1 at $t \sim 18\ P_{\rm orb}$ (the corresponding snapshots, not shown here, are very similar to those at $t = 30\ P_{\rm orb}$) and is equal to $\sim 0.6c_s$ (c_s is the sound speed for the initial surface temperature of the secondary).

At the end of the outburst, the residual flow decays due to numerical dissipation on a time scale shorter than the recurrence time of outbursts. Physical viscosity (e.g. due to turbulence) would likely bring the velocity field to zero before the start of the next outburst.

Matter is therefore transported toward the L_1 point at least during the first half of the outburst. However, Fig. 2 shows that the temperature field remains unperturbed by the flow, and no heat advection occurs. This is easily explained by considering the corresponding time scale: our numerical simulations show that the time needed for the flow to cross the shadowed region is a few orbital periods. For comparison, the cooling timescale of the gas is:

$$\tau_{\rm cool} = \frac{\Sigma c_v T}{\sigma T^4} \propto \Sigma T^{-3} \tag{3.1}$$

In these low mass stars, the surface density of the layer affected by irradiation is of order of ~ 100 g.cm^{-2}. Due to the strong temperature dependence, the cooling time scale of the hot gas ($T \sim 10^4$ K) is never larger than $\sim 0.1P_{\rm orb}$. This is much shorter than the crossing time scale and no heat can be efficiently transported toward L_1.

4 Mass transfer enhancement ?

The rate at which matter leaves the secondary is given by (see Lubow & Shu 1975, Meyer & Meyer-Hofmeister 1983):

$$\dot{M} = Q\rho(L_1)c_s \tag{4.1}$$

where Q is the cross section of the stream, $\rho(L_1)$ is the gas density at L_1 and c_s is the isothermal sound speed L_1. The Qc_s yields a $T(L_1)^{3/2}$ dependence of the mass transfer rate on the temperature at L_1. If we further assume that vertical hydrostatic equilibrium is a good approximation, $\rho(L_1)$ also depends on $T(L_1)$ (likely more drastically than Qc_s). As we have shown that the temperature at L_1 is unchanged, this would imply that no mass transfer enhancement occurs.

However, just beneath L_1 the Coriolis force is in the vertical direction. The Coriolis force then acts as a negative effective gravity and modifies the vertical hydrostatic balance:

$$\frac{dP}{dz} = -\rho g(z) + \rho 2\Omega v_\parallel = -\rho g_{\rm eff} \tag{4.2}$$

where the z axis is the local vertical axis, $g(z)$ is the Roche gravity and $v_{\parallel}$ is the surface velocity of the gas. Due to the Coriolis force, the point were the effective gravity vanishes is below L_1. In this case, one should replace $\rho(L_1)$ in Eq. (4.1) by the density at the point where the effective gravity vanishes.

Since we do not know the vertical profile of $v_{\parallel}$, we solved Eq. (4.2) with an uniform $v_{\parallel} = 0.5, 0.75, 1.0 c_s$. The results are shown in Fig. 3. In this case the mass transfer enhancement is directly given by the increase of density. Our results depend on the ratio z_{L_1}/H (i.e. the altitude of L_1 measured in units of pressure heigth scale of the atmosphere). This ratio has to be determined by computing the vertical structure of the atmosphere, which is beyond the scope of this study. We consider in Fig. 3 two cases: $z_{L_1}/H = 1.2$ and $z_{L_1}/H = 2$. The mass transfer enhancement is moderate.

Finally, it should be noted that as the velocity reaches a fraction of the sound speed, it is possible that the hydrostatic equilibrium assumption breaks in the whole vertical extend of the layer. A detailed analysis would require 3D simulations which are out of the scope of this study.

5 Conclusion

The adjustment of a fluid to a pressure perturbation (in our case triggered by irradiation) when the dynamic is dominated by the Coriolis force is not an easy problem and is known by meteorologists under the name of "geostrophic adjustment" (see e.g. Pedlosky 2003). The assumption of steady state in previous studies is therefore incorrect. We have shown that contrary to naive expectations, a circulation flow toward L_1 forms thanks to the Coriolis force. Despite the strength of the flow at L_1, which can reach a fraction of the sound speed, no heat is effectively transported. This due to the quick radiative cooling which occurs in our model, on a typical time scale of 0.1 $P_{\rm orb}$. If hydrostatic equilibrium is a good approximation in the L_1 region, only the Coriolis force could lead to a moderate increase of the mass transfer (by a factor of a few), probably not large enough to significantly affect the DN outburst. It also remains possible that hydrostatic equilibrium breaks down in the whole vertical extent, but in this case a 3D approach is needed to determine the mass flux leaving the secondary.

Finally, note that even if one of the above mentioned effects leads to a mass transfer enhancement episode, it would not last longer than $10 - 20$ orbital periods, as the anti-cyclonic perturbation drifts westwards thus quenching the flow through L_1 on the same time scale.

References

Cannizzo, J.K. 1993, in Accretion Disks in Compact Stellar Systems, World Scientific

Hameury, J.-M., Menou, K., Dubus, G., Lasota, J.P., & Hure, J.M. 1998, MNRAS, 298, 1048

Hameury, J.-M. 2000, New Astronomy Reviews, 44, 15

Kopal, Z 1969, Ap&SS, 5, 360

Lasota, J.-P. 2001, New Astronomy Reviews, 45, 449

Meyer, F., & Meyer-Hofmeister, E. 1983, A&A, 121, 29

Lubow, S.H., & Shu, F.H. 1975, ApJ, 198, 383

Osaki, Y., & Meyer, F. 2003, A&A, 401, 325

Osaki, Y., & Meyer, F. 2004, A&A, 428, 17

Pedlosky, J. 1982, Geophysical Fluid Dynamics, Springer

Pedlosky, J. 2003, Waves in the Ocean and Atmosphere, Springer

Smak, J. 1995, AcA, 45, 355

Smak, J. 1999, AcA, 49, 391

Smak, J. 2000, New Astronomy Reviews, 44, 171

Smak, J. 2004a, AcA, 54, 181

Smak, J. 2004b, AcA, 54, 221

Smak, J. 2004c, AcA, 54, 429

Viallet, M., Hameury, J.-M. 2007, A&A

Warner, B. 1995, Catacysmic Variable stars (Cambridge Univ. Press)

Yee, H.C. 1987, NASA Technical Memorandum 89464